

Journal Pre-proofs

Research paper

A polyoxometalate supported copper dimeric complex: Synthesis, structure and electrocatalysis

N. Tanmaya Kumar, Umashis Bhoi, Pragya Naulakha, Samar K. Das

PII: S0020-1693(19)31797-9
DOI: <https://doi.org/10.1016/j.ica.2020.119554>
Reference: ICA 119554

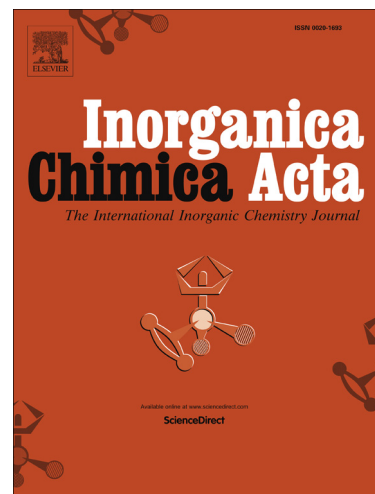
To appear in: *Inorganica Chimica Acta*

Received Date: 20 November 2019
Revised Date: 23 February 2020
Accepted Date: 24 February 2020

Please cite this article as: N.T. Kumar, U. Bhoi, P. Naulakha, S.K. Das, A polyoxometalate supported copper dimeric complex: Synthesis, structure and electrocatalysis, *Inorganica Chimica Acta* (2020), doi: <https://doi.org/10.1016/j.ica.2020.119554>

This is a PDF file of an article that has undergone enhancements after acceptance, such as the addition of a cover page and metadata, and formatting for readability, but it is not yet the definitive version of record. This version will undergo additional copyediting, typesetting and review before it is published in its final form, but we are providing this version to give early visibility of the article. Please note that, during the production process, errors may be discovered which could affect the content, and all legal disclaimers that apply to the journal pertain.

© 2020 Published by Elsevier B.V.



A polyoxometalate supported copper dimeric complex: Synthesis, structure and electrocatalysis

N. Tanmaya Kumar,^a Umashis Bhoi,^a Pragya Naulakha^b and Samar K. Das^{a*}

^a School of Chemistry, University of Hyderabad, Prof. C. R. Rao Road, Gachibowli, Hyderabad, Telangana, India 500046

^b School of Physical Sciences, Jawaharlal Nehru University, New Delhi, India 110067

Abstract. A polyoxometalate (POM) supported copper dimeric complex, $[\text{Mo}_8\text{O}_{26}\{\text{Cu}_2(2,2'\text{-bpy})_2(\text{CH}_3\text{COO})_2\text{H}_2\text{O}\}_2] \cdot \text{H}_4\text{Mo}_8\text{O}_{26} \cdot 16\text{H}_2\text{O}$ (**1**) has been synthesized using conventional wet synthesis. The compound has been characterized using routine spectral techniques and its molecular structure has been elucidated using single crystal X-ray crystallography. The two copper(II) ions are bridged by acetate ions and each copper ion is also coordinated to 2,2'-bipyridine molecule. In each dimer, one of the copper ions is bonded to the POM anion from one side, whereas the other copper ion is bonded to a water molecule, hence acquiring a penta-coordinated square pyramidal structure around each copper center. The lattice water molecules play an important role to stabilize the system, by forming a water pentamer, which binds both the polyoxometalate supported transition metal complex and the other POM anion $[\text{Mo}_8\text{O}_{26}]^{4-}$. Interestingly, compound **1** is found to function as a versatile heterogeneous electro-catalyst for water oxidation, proton reduction and hydrogen peroxide reduction.

1. Introduction

Polyoxometalates (POMs) are interesting transition metal oxide clusters, that have grabbed the attention of the contemporary scientists, because of their structural versatility and their applicability in a vivid range of areas ranging from catalysis, materials sciences, biology, magnetism, luminescence to molecular electronics through medicine.¹ A recent modification to the polyoxometalates is the introduction of the coordination complexes into the framework by covalently grafting the complex through the terminal / bridging oxygen atom(s) of the polyoxometalates, taking into consideration the charge compensation or the structure direction, which are called polyoxometalate supported transition metal complexes (PSTMCs).² This modification enhances the potential applications of these hybrid PSTMCs in many diverse fields.³

Copper ions play a major role in biological processes. Among the copper containing metalloenzymes, hemocyanins (found in mollusks) are oxygen carriers. These hemocyanins contain a copper dimer, which is bridged by the oxygen atoms. Many modeling studies have been done, so far, in order to mimic the functional as well as the structural aspects of the copper dimeric complexes in copper metalloenzymes.⁴ Melnik and co-workers in the year 1997,⁵ published a review reporting more than nine hundred types of Cu(II) dimers, which evidences the importance and applicability of this family of compounds. According to this review, the earliest quotation to copper acetate was from the year 1594.⁵ The review⁵ also generalizes the fact that, as far as the stereochemistry of these dimeric compounds is concerned, they favor a square pyramidal geometry with different degrees of distortions about the Cu(II) ion. In the last two decades, there has been an extensive study on the reactivity of tetra- μ -

acetatodicopper(II) towards the 2,2'-bipyridine (bpy). In 1992, Perlepes and co-workers reported the isolation of $[\text{Cu}_2(\mu\text{-O}_2\text{CMe})_2(\text{H}_2\text{O})_2(\text{bpy})_2](\text{ClO}_4)_2 \cdot \text{H}_2\text{O}$ from the reaction of $[\text{Cu}_2(\text{OH})_2(\text{bpy})_2]\text{ClO}_4$ with an excess of MeCO_2H .⁶ Followed by this report, Chakravarty and Meenakumari reported the synthesis and crystal structure of $[\text{Cu}_2(\mu\text{-O}_2\text{CMe})_2(\text{H}_2\text{O})(\text{bipy})_2](\text{PF}_6)_2$, where the two Cu(II) ions exhibited two different coordination geometries.⁷

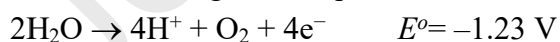
In the present work, we have synthesized the polyoxometalate supported dimeric transition metal complex $[\text{Mo}_8\text{O}_{26}\{\text{Cu}_2(2,2'\text{-bpy})_2(\text{CH}_3\text{COO})_2\text{H}_2\text{O}\}_2] \cdot \text{H}_4\text{Mo}_8\text{O}_{26} \cdot 16\text{H}_2\text{O}$ (**1**).

Prior to this work, there are few reports on copper dimeric complexes supported on diverse polyoxometalates (POMs). Gutiérrez-Zorrilla, Lezama and their co-workers have done enormous work in this field, i.e., POM supported dimeric copper complex. They reported a unique dinuclear copper complex, supported on a Keggin type of polyoxometalate $\text{K}_{14}[\{\text{Cu}_2(\text{bpy})_2(\mu\text{-ox})\}\{\text{SiW}_{11}\text{O}_{39}\text{Cu}(\text{H}_2\text{O})\}]_2[\text{SiW}_{11}\text{O}_{39}\text{Cu}(\text{H}_2\text{O})] \cdot \sim 55\text{H}_2\text{O}$.⁸ Subsequently, they depicted a full account of this work describing variable temperature magnetic studies.⁹ In yet another report, they also reported reaction of a monosubstituted Keggin polyoxometalate (POM) generated *in situ* with copper-phenanthroline complexes, where the two Keggin cluster anions are connected through a terminal oxygen atom yielding $\text{A}_7[\text{Cu}_2(\text{ac})_2(\text{phen})_2(\text{H}_2\text{O})_2][\text{Cu}_3(\text{ac})_3(\text{phen})_3(\text{H}_2\text{O})_3][\text{Si}_2\text{W}_{22}\text{Cu}_2\text{O}_{78}(\text{H}_2\text{O})] \cdot \sim 18\text{H}_2\text{O}$, where $\text{A} = \text{NH}_4^+$ or Rb^+ .¹⁰ A little later, the same groups described two interesting POM supported copper dimeric compounds, where the second one is the condensed dimer of the first one.¹¹ In the

next year, they also reported the reaction of *in situ* generated copper(II)-monosubstituted Keggin polyoxometalates and copper(II)-phenanthroline-oxalato complexes in ammonium or rubidium acetate buffers leading to the formation of two new hybrid POMs, where the dinuclear copper-oxalato complex is sandwiched by two copper-monosubstituted POMs $\text{E}_4[\text{Cu}(\text{phen})(\text{H}_2\text{O})_4]_2[\text{Cu}_4(\text{phen})_4(\text{H}_2\text{O})_4(\text{ox})_3]_{0.6}[\text{Cu}_2(\text{phen})_2(\text{H}_2\text{O})_4(\text{ox})]_{0.4}[\text{Cu}(\text{phen})(\text{ox})]_{0.8}[\{\text{SiW}_{11}\text{O}_{39}\text{Cu}(\text{H}_2\text{O})\}_2\{\text{Cu}_2(\text{phen})_2(\text{ox})\}] \cdot 20\text{H}_2\text{O}$ [$\text{E}: \text{Rb}^+$ or NH_4^+].¹² Ma and coworkers reported a one dimensional polyoxometalate-based chain, constructed from Keggin anions of $[\text{SiMo}_{12}\text{O}_{40}]^{4-}$ weakly connected by dinuclear $[\text{Cu}(\text{ppy})_2]$ groups. The two copper atoms are connected to two terminal oxygen atoms of two different Keggin atoms, forming a planar rhombic copper dimer.¹³ Wang and group reported reduced tungsten Keggin supported chloro-bridged copper dimers including related supramolecular chemistry.¹⁴ Ma, Liu and co-workers reported the hydrothermal synthesis of a hybrid POM complex, $[\text{Cu}_2(\text{bipy})_3(\mu_1\text{-H}_2\text{O})_2(\mu_2\text{-H}_2\text{O})(\mu_2\text{OH})(\text{H}_2\text{BW}_{12}\text{O}_{40})] \cdot 4\text{H}_2\text{O}$ (bipy = 4,4'-bipy) having a Cu dimer connected to 4, 4'-bipyridine from one side and the terminal oxygen of the cluster from the other side. The two copper ions are bridged by water molecules and showed the existence of weak anti-ferromagnetic interactions.¹⁵ A similar complex was also reported by Ma and Pang, where the POM was $[\text{PW}_{12}\text{O}_{40}]^{n-}$.¹⁶ Zhao and group have described (hydroxo)(chloro) bridged copper dimer, supported by the silicotungsten Keggin in compound $[\text{Cu}_2(\text{phen})_2\text{Cl}(\text{H}_2\text{O})(\text{OH})]_2[\alpha\text{-SiW}_{12}\text{O}_{40}] \cdot 8\text{H}_2\text{O}$.¹⁷ Ma, Pang and their co-workers reported two copper dimeric-

POM complexes
 $\{[\text{Cu}_2(\text{en})_2(\text{ox})][\text{HPW}_{12}\text{O}_{40}]\} \cdot (\text{en})_2 \cdot 2\text{H}_2\text{O}$
 and $\{[\text{Cu}_2(\text{en})_2(\text{ox})][\text{H}_3\text{BW}_{12}\text{O}_{40}]\} \cdot (\text{en})_2 \cdot 2\text{H}_2\text{O}$.¹⁸ Xu and co-workers,¹⁹ have reported a similar PSTMC $[\text{Cu}(\text{bpy})(\mu_2\text{-OH})]_4[(\text{H}_2\text{O})\text{-}(\text{bpy})_2\text{HPW}_{11}\text{Cu}_2\text{O}_{39}]_2 \cdot 2\text{C}_2\text{H}_5\text{OH} \cdot 10\text{H}_2\text{O}$, where the Cu(II) ions are located in the lacunary sites of the monolacunary anion $[\text{PW}_{11}\text{O}_{39}]^{7-}$ forming a dumbbell type structure.

Even though these impactful reports have brought about structural aesthetics and interesting magnetism on these polyoxometalate supported copper dimeric complexes, their use as electro-catalysts is scarcely reported. Ma, Pang and co-workers have reported the role of copper dimer, supported on polyoxometalates as electrocatalysts for the reductions of hydrogen peroxide, potassium iodate and nitrite.¹⁸ There are not many reports on electrocatalytic water oxidation and electrocatalytic proton reduction, catalyzed by POM supported copper dimers, that are enormously important today because the water splitting (WS) process using an inexpensive POM-based catalyst is a powerful alternative to curb the energy crisis on the earth surface. Water oxidation (WO) is considered to be the bottleneck process of water splitting because it advances in a thermodynamically uphill manner with the involvement of 4e^- and 4H^+ ,²⁰ according to the equation:



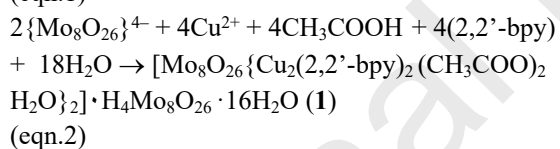
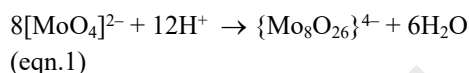
where E° is the standard Nernst potential for water oxidation; here a negative potential signifies the thermodynamic uphill nature of the process. Our group has reported a nickel coordination complex, attached to a polyoxometalate cluster anion, to be a robust electrocatalyst for water oxidation process.²¹

The present years have also seen an ample interest to design new molecular catalysts, containing earth-abundant 3d-transition metals as the active site for electrocatalytic hydrogen evolution reactions. Nickel,²² cobalt²³ and iron²⁴ based complexes are few popular molecular catalysts, which have been employed in electrocatalytic hydrogen evolution reactions (HER). In 2014, Wang and co-workers, for the first time, reported a Cu-complex that can electrochemically catalyze water reduction^{25a} with a very high catalytic activity with 96% Faradic efficiency and 420 mV onset overpotential in pH 2.5 under buffer conditions. After this report, many Cu-based complexes were discovered, which showcased activity in catalyzing HER electrochemically.²⁵ Recently, our group has described two Anderson-POM supported copper complexes acting as electrocatalysts for hydrogen evolution reaction in neutral medium.²⁶ The electrocatalytic proton reduction to molecular hydrogen has attracted immense attention because the molecular hydrogen (H_2) is a clean and highly efficient fuel. Likewise, since hydrogen peroxide is commonly used as an oxidant in chemical mechanical planarization slurries leading to the metallization of copper for microelectronics applications, the electrocatalytic reduction of H_2O_2 by copper-containing catalyst is utmost demanding. In this article, we have demonstrated that the synthesized polyoxometalate supported dimeric copper complex $[\text{Mo}_8\text{O}_{26}\{\text{Cu}_2(2,2'\text{-bpy})_2(\text{CH}_3\text{COO})_2\text{H}_2\text{O}\}_2] \cdot \text{H}_4\text{Mo}_8\text{O}_{26} \cdot 16\text{H}_2\text{O}$ (**1**) can be used as a versatile heterogeneous catalyst for electrochemical water oxidation, proton reduction, and hydrogen peroxide reduction in acidic medium.

2. Results and Discussion

2.1 Synthesis

Compound **1** was synthesized following a one-pot conventional wet synthesis protocol at 70 °C. The blue-colored filtrate yielded 0.8 g (20.3% based on Mo) blue block crystals within four days. The relevant synthesis includes the reaction of sodium molybdate, 2,2'-bipyridine, $\text{Cu}(\text{NO}_3)_2 \cdot 6\text{H}_2\text{O}$ and CH_3COONa in an aqueous acidic medium. The sodium molybdate solution, when acidified with glacial acetic acid immediately gives a white precipitate of $[\text{Mo}_8\text{O}_{26}]^{4-}$, which upon addition of $\text{Cu}(\text{NO}_3)_2 \cdot 6\text{H}_2\text{O}$ and CH_3COONa coordinates to Cu(II) through its terminal oxygen atom. Looking at the formula of **1**, the following reactions can be proposed during the synthesis of compound **1**:



The tetrahedral molybdate $[\text{MoO}_4]^{2-}$ in an acidic aqueous solution undergoes protonation followed by coordination expansion around molybdenum and subsequent condensation reaction results in the formation of the isopolyanion $\{\text{Mo}_8\text{O}_{26}\}^{4-}$, as shown in eqn. 1. Subsequently, the *in-situ* formed $\{\text{Mo}_8\text{O}_{26}\}^{4-}$ acts as the ligand through its terminal oxo donor to coordinate to one of the copper centres of each copper dimer (there are two such copper dimers per one POM cluster anion, formed *in situ* from the copper(II) salt, acetate anion and 2,2'-bipyridine (eqn. 2)).

The detailed synthetic procedure is provided in the Experimental Section. The powder X-ray diffraction (PXRD) pattern, generated from CIF file of single-crystal data of compound **1** (simulated PXRD pattern), matches well with that, obtained from the bulk PXRD measurement of the sample (*vide infra*). This confirms the purity in the bulk sample.

2.2 Crystallography

The asymmetric unit of compound **1** consists of two halves of the octamolybdate anions, one copper acetate dimer, and eight lattice water molecules (Fig. 1a). Thus the full molecule contains two POM clusters, two copper dimers, and sixteen solvent water molecules as shown in Fig. 1b. An octamolybdate anion, $[\text{Mo}_8\text{O}_{26}]^{4-}$ consists of eight edge-sharing octahedral $\{\text{MoO}_6\}$ units. The Mo–O bond distances can be grouped into four categories: 14 Mo–O_t (O_t = terminal oxygen) with the bond lengths in the range of 1.686–1.706 Å; six μ_2 -type bridged Mo–O_b (O_b = bridging oxygen) with bond distances in the range of 1.740– 2.295 Å; four μ_3 -type bridged Mo–O_b bonds in the range of 1.984–2.329 Å and two μ_5 -type Mo–O_b bonds (2.155 and 2.402 Å). The polyhedral representation of the POM clusters is shown in Fig. 1c.

In the crystal structure, there are two independent POM cluster $[\text{Mo}_8\text{O}_{26}]^{4-}$ anions. One of these, supports two copper dimers *via* terminal Mo=O coordination resulting in the formation of POM supported copper dimeric complexes,

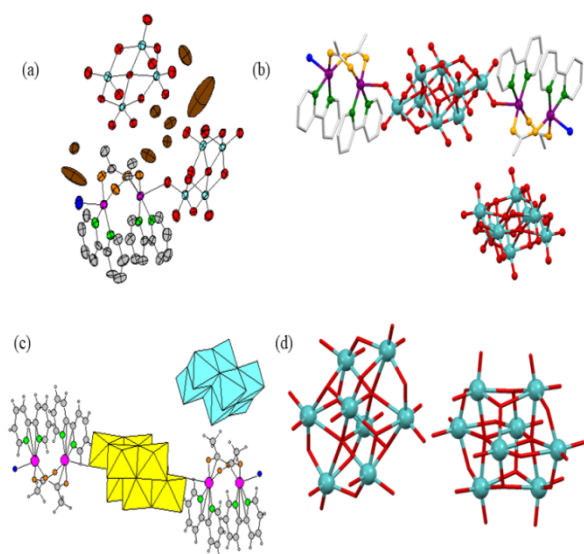


Fig. 1. (a) The thermal ellipsoidal plot of compound **1** at the 50% probability level. Hydrogen atoms are omitted for clarity. (b) The full molecule of **1** excluding the lattice water molecules. (c) Polyhedral representation of the POM clusters in compound **1** excluding the water molecules. (d) Two independent cluster anions of $[\text{Mo}_8\text{O}_{26}]^{4-}$ polyoxometalate, showing their β conformation. Color code: Cyan: molybdenum; Red: oxygen atoms of the octamolybdate cluster anion; violet: copper; grey: carbon; orange: oxygen atoms of acetate ions; green: nitrogen; blue: water molecule attached to the copper dimer; brown: lattice water molecules; white: hydrogen.

$[\text{Mo}_8\text{O}_{26}\{\text{Cu}_2(\text{CH}_3\text{COO})_2(\text{bpy})_2(\text{H}_2\text{O})\}_2]$ and other POM cluster remains as a lattice component as a proton salt along with sixteen lattice water molecules per formula unit, thereby giving the overall formula of the title compound as $[\text{Mo}_8\text{O}_{26}\{\text{Cu}_2(2,2'\text{-bpy})_2(\text{CH}_3\text{COO})_2\text{H}_2\text{O}\}_2]\text{H}_4\text{Mo}_8\text{O}_{26}\cdot 16\text{H}_2\text{O}$ (**1**). Each copper (Cu^{II}) dimeric complex is connected to the $[\text{Mo}_8\text{O}_{26}]^{4-}$ cluster through an apical position of the copper complex. The copper dimeric complex comprises of two square-pyramidal $\text{Cu}(\text{II})$ atoms bridged by two acetic acid ligands in a *syn-syn* fashion with a $\text{Cu}-\text{Cu}$ distance of 3.007 Å. The basal plane is occupied by two bipyridine N atoms and O atoms from the acetate ions

with the apical position being coordinated to one of the terminal oxygen atoms of the octamolybdate for one $\text{Cu}(\text{II})$ ion and water to another $\text{Cu}(\text{II})$ ion. Overall, in the POM supported copper dimer complex system, $[\text{Mo}_8\text{O}_{26}\{\text{Cu}_2(\text{CH}_3\text{COO})_2(\text{bpy})_2(\text{H}_2\text{O})\}_2]$, the isopolyanion is covalently bonded to two copper dimeric complexes $[\text{Cu}_2(\text{CH}_3\text{COO})_2(\text{bpy})_2(\text{H}_2\text{O})]^{4+}$ from opposite sides. The β conformation of the POM clusters, stabilized in compound **1**, is shown in Fig. 1d that shows octahedral coordination of each molybdenum centre in $\{\text{Mo}_8\text{O}_{26}\}^{4-}$.²⁷

The detailed crystal structure analysis of compound **1** shows that the POM anion, coordinating copper dimers, interacts with a crystallographically independent POM cluster, remaining as a lattice component as an acid salt $\text{H}_4\text{Mo}_8\text{O}_{26}$, *via* a supramolecular cyclic water pentamer $(\text{H}_2\text{O})_5$. The water pentamer is an open envelope-shaped, as determined crystallographically in compound **1**. The five water molecules, involved, are the four lattice water molecules and the water, coordinated to the copper atom (Fig. SI S1). The relevant $\text{O}\cdots\text{O}$ separations in the water pentamer, $(\text{H}_2\text{O})_5$ are: $\text{O}18\cdots\text{O}36$: 2.731Å; $\text{O}36\cdots\text{O}37$: 2.809Å; $\text{O}37\cdots\text{O}32$: 2.792Å; $\text{O}32\cdots\text{O}33$: 2.978Å; $\text{O}33\cdots\text{O}18$: 2.871Å.

Besides the stabilization of a water pentamer, there also exist the $\text{C}-\text{H}\cdots\text{O}$ hydrogen bonding interactions which contribute to stabilizing the supramolecular chainlike arrangement in the crystal structure of compound **1**, as shown in Fig. 2. The $-\text{CH}-$ groups of the carbon atoms C1, C2, C3, C4, C9, C10, C11, C12, C14, C19, C20, C22 and C24 donate their hydrogens to the surrounding

available possible surface sites of the octamolybdate cluster anion (that include bridging and terminal oxygen atoms), (SI, Fig. S2).

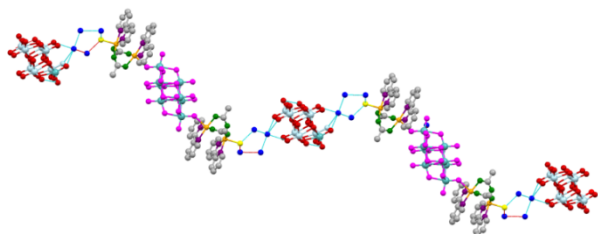


Fig. 2. The chain-like structure formed through hydrogen bonds between the dimeric complex, the lattice octamolybdate cluster, and the water pentamers, (hydrogen atoms are not shown for clarity).

The π - π stacking interactions in the compound **1** are also studied. Since there are four bipyridine ligands connected to the four copper(II) centres, each bipyridine ligand faces the other one, in a dimeric pair. As can be seen in Fig. S3, the centroids of each pyridine ring pair are at a distance of 3.615 and 3.677 Å. These pyridine rings are slip-stacked to each other and not completely sandwiched, as the later leads to less stable compound, on account of high electronic repulsion of the electrons in the π -orbitals of the pyridine rings.

2.3 Spectroscopy

The Fourier transformed infrared spectrum of the compound **1** was recorded. (Fig. S4) The strong peak at 938 cm^{-1} can be attributed to the asymmetric stretch of the Mo–O_t bond. Similarly, the asymmetric stretch of Mo–O_b–Mo bond is found to be seen at 724 cm^{-1} . The peaks at 724, 766, 838 and 893 cm^{-1} are the characteristic peaks for Mo–O_b asymmetric stretch. All these values almost match with the vibrational features, reported for the β -

Table 1 Crystal data and structure refinement for compound **1**

| | Compound 1 |
|--|---|
| Empirical formula | C ₄₈ H ₄₄ Cu ₄ Mo ₁₆ N ₈ O ₇₈ |
| fw | 3770.16 |
| $T(\text{K}), \lambda(\text{Å})$ | 273(2), 0.71073 |
| Crystal system | Triclinic |
| Space group | $P-1$ |
| a (Å) | 12.135(3) |
| b (Å) | 12.766(3) |
| c (Å) | 19.016(5) |
| α (°) | 104.490(8) |
| β (°) | 98.770(9) |
| γ (°) | 111.063(8) |
| V (Å ³) | 2564.0(11) |
| Z, d_{calcd} (g cm ³) | 1, 2.442 |
| μ (mm ⁻¹), $F(000)$ | 2.808, 2139.0 |
| goodness-of-fit on F^2 | 1.407 |
| $R1$ | 0.0728 |
| $wR2$ | 0.3005 |
| Largest diff. peak/hole (e Å ⁻³) | 2.6 |

isomer of the octamolybdate in the literature.²⁸ The vibrational features of compound **1** in two different ranges are

given in SI (Figs S4 and S5), which clearly show the characteristics of the β -isomer of the octamolybdate. The presence of the water molecules in the compound is evident from the broad peak around 3000 cm^{-1} . The peaks at 3520 and 3460 cm^{-1} are attributed to the symmetric stretch corresponding to the water molecules bonded to the Cu(II) ions. Similarly, the broad peak at 2950 cm^{-1} is for the symmetric stretch of the CH_3 groups of the acetate ions. The bands at 1600 and 1577 cm^{-1} can be attributed to the asymmetric stretch of the COO^- group and at 1441 and 1428 cm^{-1} for its symmetric stretch (Fig. S5, SI). The peak at 1636 cm^{-1} is for the C=C bond of the bipyridine ligand. Other peaks at 1577, 1428, 1312, 1254, 1035 and 1020 cm^{-1} can be attributed to the various vibrational features of the bipyridine ligands.²⁹

The electronic absorption spectrum of compound **1** is transformed into a Kubelka-Munk (K-M) derived plot as shown in Fig. S6a, SI. The sharp peak at 226 nm can be ascribed to the ligand to metal charge transfer from the oxygen $2p$ to the molybdenum d orbital.³⁰ The shoulder at 271 nm can be attributed to the intra-ligand bipyridine π - π^* transitions. The broad peak centred around 467 nm can be attributed to the d to π^* transitions.³¹ A diffused broad peak is also seen at around 350 nm, which can be attributed to the acetate to copper LMCT.³² A broad and weak peak is also seen around 600 nm, which is due to d - d transitions of the d^9 Cu(II) center in the title compound.

The thermal stability of the title compound has been studied by thermogravimetric analysis. The compound was taken for thermal studies

without prior activation in a high-temperature vacuum. With an increase in temperature from 30 °C to nearly 240 °C, as shown in Fig. S6b, SI, there is a weight loss, which can be attributed to the loss of lattice water molecules as well as the water molecules coordinated to the Cu(II) ion. Followed by this, there is a weight loss of up to nearly 62% of the weight when the temperature increases from 240 °C to 380 °C. In this temperature range, the four acetate ligands and four bipyridine ligands of the copper dimers are lost leaving the octamolybdate clusters and the copper contents. Then after 750 °C, the polyoxometalate clusters and the copper content start to degrade into their oxides.

2.4 Electrochemical Studies

The electrochemical responses of compound **1** were studied in various electrolytes. The responses in different electrolytes, as expected, were different. As we know that the $[\text{Mo}_8\text{O}_{26}]^{4-}$ cluster is stable in aqueous solution in pH less than 5.5 and is transformed to paramolybdic anions in pH 5.5 to 8,³³ hence all the electrochemical studies were performed in pH less than 5.5. The cyclic voltammetric studies were done in various electrolytes and at various pH values.

The cyclic voltammograms of compound **1** in 0.1M phosphate buffer and 0.1M Na_2SO_4 solution at different pH values are shown in Fig. 3. The compound shows similar redox responses at different pH values (except at pH 4 in 0.1M phosphate buffer) in both the electrolytes. A quasi-reversible redox couple, that has appeared as a major redox response in all the cases (except at pH 4 in 0.1M phosphate buffer), can be attributed to the $\text{Cu}^{\text{II}}/\text{Cu}^{\text{I}}$ couple. In Na_2SO_4 solution, at pH

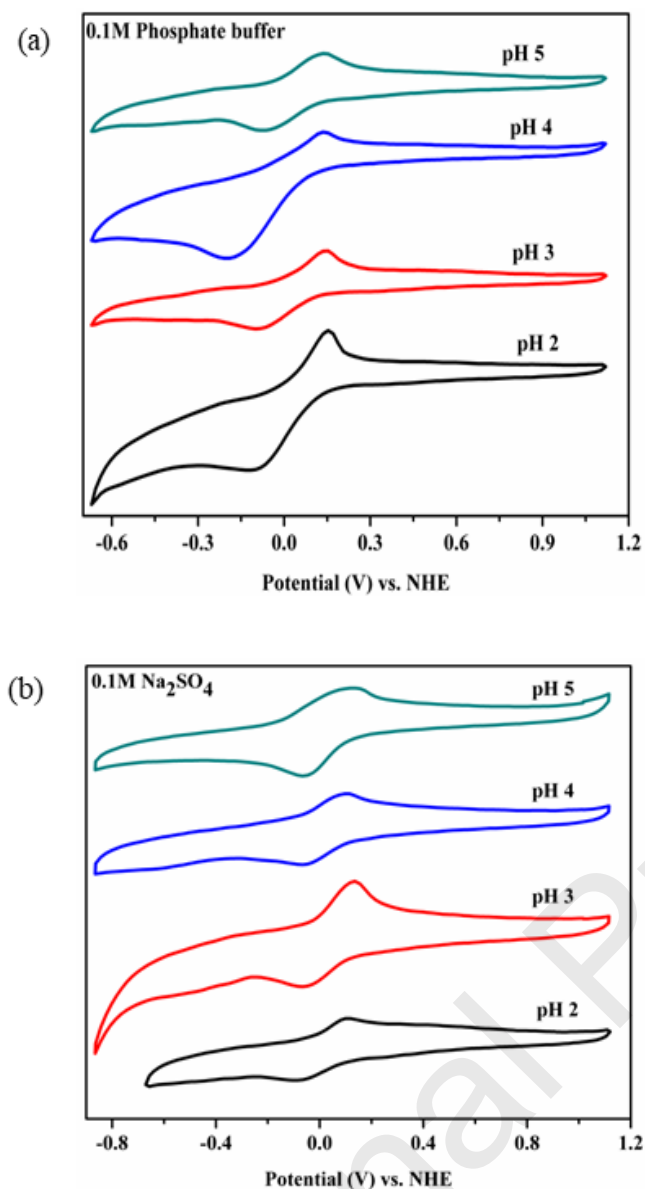


Fig. 3. Cyclic Voltammograms of compound **1** at various pH values in (a) 0.1M phosphate buffer and (b) 0.1M Na₂SO₄, at a scan rate of 100 mVsec⁻¹.

3, a careful observation reveals a weak reduction feature at -0.4V, which can be attributed to the reduction of Mo^{VI} to Mo^V of the cluster, based on the weak redox responses appeared for the precursor compound [Bu₄N]₄[Mo₈O₂₆] in 0.1M Na₂SO₄ at pH 5 as shown in Fig. 4. The voltammograms at varied scan rates in different electrolytes (at different pH values) are given in supplementary information (Fig. S9, SI). Table S1 (SI)

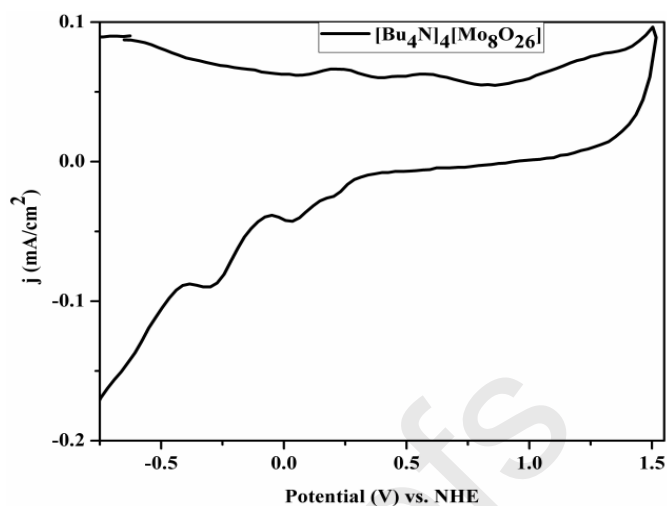


Fig. 4. Cyclic Voltammogram plot of [Bu₄N]₄[Mo₈O₂₆] in 0.1M Na₂SO₄ at pH 5 at a scan rate of 100 mVsec⁻¹.

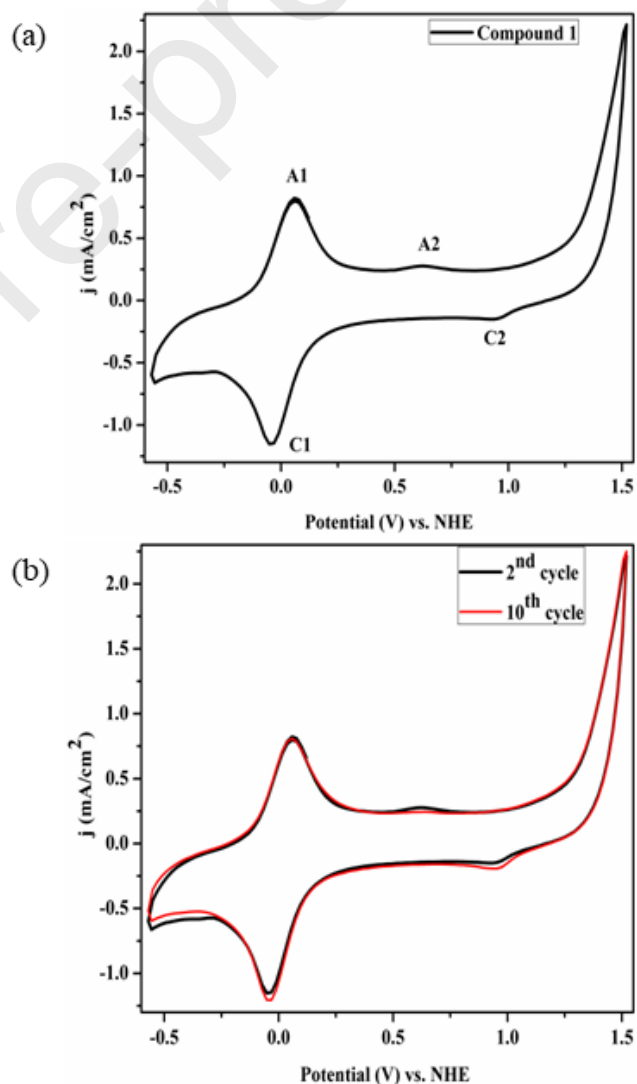


Fig. 5. (a) Cyclic voltammogram of compound **1** in 0.1M KCl. (b) The water oxidation activity of compound **1** after 10 cycles.

gives the $E_{1/2}$ values of the compound at different pH values

2.5 Electrocatalytic water oxidation

We tested the activity of compound **1** in 0.1M KCl solution and the results, so obtained, are given in Fig. 5.

As can be seen from Fig. 5a, the increase in the current at around 1.27 V signifies the electrocatalytic water oxidation process. The reversible couple A1/C1 (E_{A1} = 0.063 V; E_{C1} = -0.05; $E_{1/2}$ = 0.0065 V vs. NHE) can be attributed to the $\text{Cu}^{\text{II}}/\text{Cu}^{\text{I}}$ couple. The activity of the compound is almost retained up to ten cycles as can be seen in Fig. 5b.

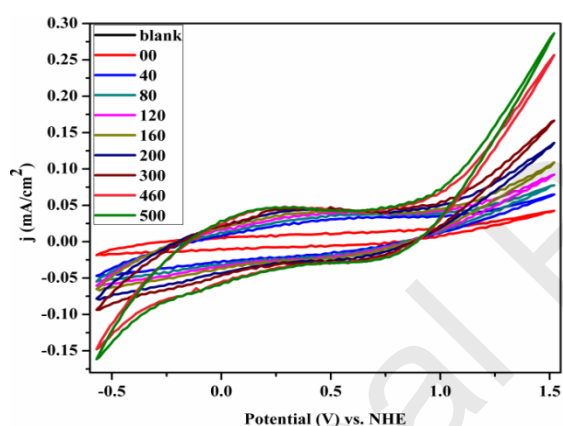


Fig. 6. Cyclic voltammogram of compound **1** in THF with $[\text{Bu}_4\text{N}][\text{BF}_4]$ as supporting electrolyte and sequential addition of water. The values in the box indicate the amount of water added to the cell in μL .

In order to assess the electrocatalytic water oxidation activity of the title compound, cyclic voltammograms of compound **1** coated glassy carbon electrode were obtained in THF, a non-aqueous solvent, with $[\text{Bu}_4\text{N}][\text{BF}_4]$ as the supporting electrolyte. This is because; we can add water sequentially (in the scale of micro-liters) to the non-aqueous reaction mixture in the electrochemical cell to investigate, whether the added water gets

oxidized electrocatalytically. The relevant voltammograms are represented in Fig. 6. As can be seen from Fig. 6, there is an increase in current in the anodic side with the sequential addition of water, with onset potential at around 0.9 V versus NHE. Thus compound **1** shows a significant electrocatalytic water oxidation response that the current intensity at around 0.9 V gradually increases with increasing amount of water. This is characteristic of electrocatalytic water oxidation. The small features, marked with A2 and C2 (Fig. 5a), can be considered as $\text{Cu}^{\text{III}}/\text{Cu}^{\text{II}}$ couple. It can be believed that the $\text{Cu}(\text{III})$ of this couple oxidizes water and comes back to its resting state, $\text{Cu}(\text{II})$, after water oxidation. The reason for the small feature of this $\text{Cu}^{\text{III}}/\text{Cu}^{\text{II}}$ couple can be explained by the fact that $\text{Cu}(\text{II})$ center with $\{\text{Cu}^{\text{II}}\text{N}_2\text{O}_3\}$ coordination with two soft donors would not be stable at its $\text{Cu}(\text{III})$ oxidation state, referring soft and hard acid-base principle.

2.6 Electrocatalytic Proton Reduction

The electrocatalytic proton reducing activity of the complex **1** was studied in 0.1M phosphate buffer, in 0.1M Na_2SO_4 at various pH values, in 0.1M KPF_6 , in 0.1M KNO_3 , in 0.1M H_2SO_4 as well as in 0.1M $[\text{Bu}_4\text{N}][\text{PF}_6]$ in acetonitrile, with acetic acid addition, in the last case. As can be seen in Fig. 7a, in 0.1M phosphate buffer, at pH 2, we get an onset at around -0.5V for electrocatalytic proton reduction and the onset goes farther towards -1V , in pH 5. As shown in Fig. 7a, the current height of electrocatalytic proton reduction increases enormously, as we go from pH 5 to pH 2. This proves that more is the number of protons (lesser the pH), more is the production of molecular hydrogen (H_2). The formation of hydrogen

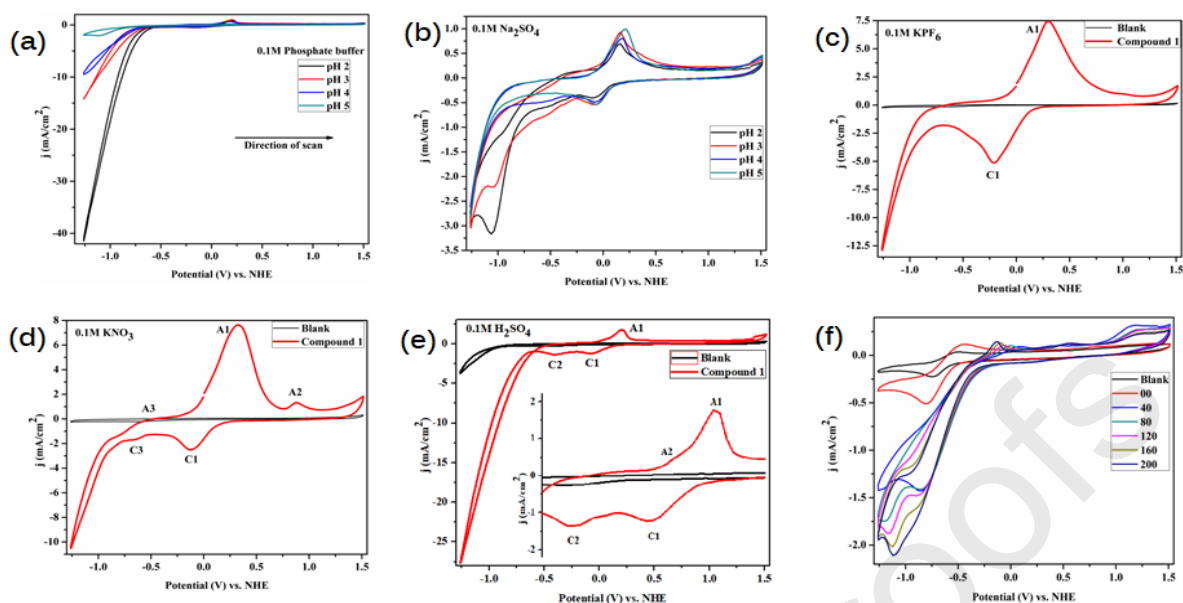


Fig. 7. Proton reduction in (a) 0.1M phosphate buffer at different pH (b) 0.1M Na_2SO_4 (c) 0.1M KPF_6 (d) 0.1M KNO_3 (e) 0.1M H_2SO_4 . In Fig. 7e the inset shows a closer view of the redox behaviour of compound **1** (f) 0.1M $[\text{Bu}_4\text{N}][\text{PF}_6]$ in acetonitrile with sequential addition of acetic acid in μL .

molecules was also evident from the visual observation of gas bubbles, found at the surface of the (working) glassy carbon electrode. In the case of 0.1M Na_2SO_4 (Fig. 7b), a similar trend is observed, i.e., with the decrease of pH, there is an increase in the amount of H_2 production. Notably, in this case, the $\text{Cu}^{\text{II}}/\text{Cu}^{\text{I}}$ couple is visible (Fig. 7b), unlike the case, where we have used phosphate buffer. Similarly, in 0.1M KPF_6 aqueous solution, along with the distinct A1/C1 couple (which can be assigned to the $\text{Cu}^{\text{II}}/\text{Cu}^{\text{I}}$ couple), we see an onset at -0.75V (Fig. 7c), which can be attributed to the electrocatalytic proton reduction to molecular hydrogen, catalyzed by compound **1**. A similar surge of current is also seen when the electrochemical reaction is carried out in 0.1M KNO_3 (Fig. 7d). The huge reduction current can be attributed to the same fact that the concerned experiment of electrocatalytic proton reduction has been performed at $\text{pH} = 1.3$. This is also evident from the hydrogen bubbles that evolved in

the cell, observed visually. Cyclic voltammograms of compound **1** in 0.1M H_2SO_4 at different scan rates (in mV/sec) are given in SI Fig. S10.

The behavior of electrocatalytic proton reduction, catalyzed by compound **1** was also performed in dry acetonitrile with continuous nitrogen gas purging with 0.1M $[\text{Bu}_4\text{N}][\text{PF}_6]$ as the supporting electrolyte (shown in Fig. 7f). In this case, we found that with the addition of acetic acid to the cell, the current intensity of the reduction at -0.6V increased and the height of this reduction peak continuously increased as acetic acid concentration was increased in the cell through sequential addition from $40\ \mu\text{L}$ to $200\ \mu\text{L}$. This continuous growth of the reduction peak is characteristic of the electrocatalytic reduction of acetic acid protons to hydrogen.

2.7 Electrocatalytic H_2O_2 reduction

The electrocatalytic reduction of hydrogen peroxide was also assessed for compound **1**. As we know that hydrogen peroxide undergoes thermal decomposition at room temperature, hence the electrocatalytic experiments were performed keeping the cell in an ice bath. The

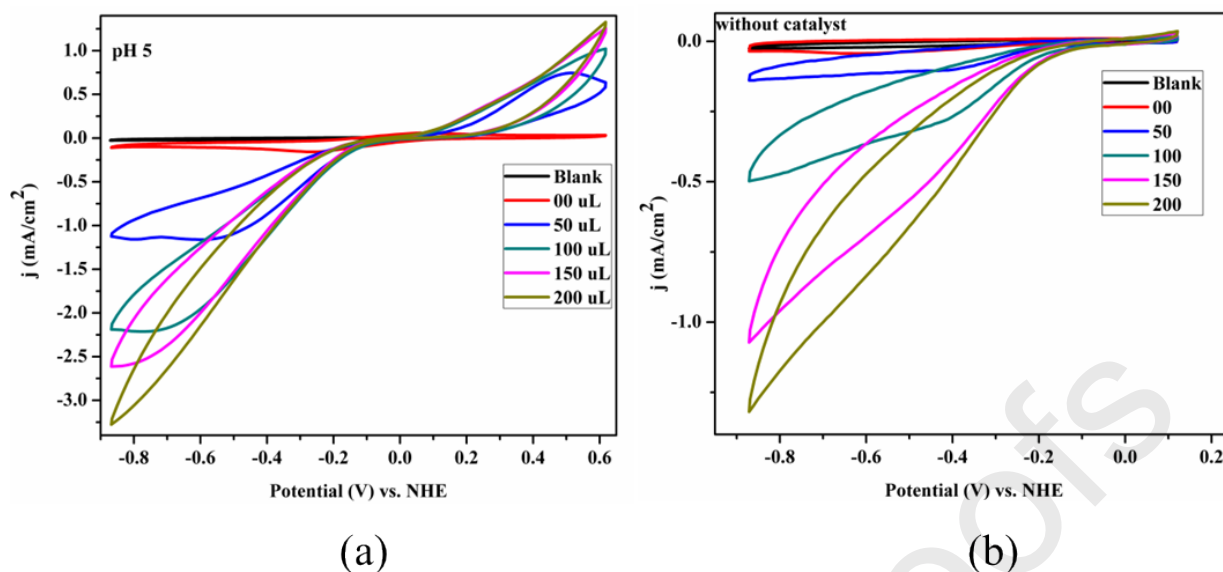


Fig. 8. The electrocatalytic hydrogen peroxide reduction (a) without and (b) with compound **1** as a catalyst in 0.1M Na₂SO₄ at pH 5.

voltammograms corresponding to the reduction of hydrogen peroxide in 0.1M Na₂SO₄ at pH 5 without and with the catalyst are shown in Fig. 8a and Fig. 8b respectively. As we can see, in both cases, the reduction peak increases with an increase in the concentration of H₂O₂. But, the role of the catalyst is clear if we see the current produced in both cases. There is a substantial increase in the reduction current in the presence of compound **1**, which proves that the compound plays the role of an electro-catalyst, which readily catalyzes the reduction of hydrogen peroxide.

3. Conclusion

Polyoxometalate (POM) supported transition metal coordination complexes are a huge group of heterogeneous compounds in the POM family. And POM supported copper dimers belong to a very small class of compounds in this family; very few members of this class exhibit electrocatalytic applications. To our knowledge, there is no report, so far, on electrocatalytic water oxidation and proton reduction, catalyzed by a POM supported

copper dimer complex. In the present article, we, not only, have demonstrated the successful synthesis and characterization of a copper dimeric complex, supported on a Keggin POM cluster anion, but also we have shown the electrocatalytic water oxidation to molecular oxygen, proton reduction to molecular hydrogen and electrocatalytic reduction of hydrogen peroxide using the synthesized POM supported copper dimeric complex.

4. Experimental Section

4.1 General Materials and Methods

All the starting materials were purchased as analytical grade and were used as received. IR spectrum of the compound was obtained on a JASCO-5300 FTIR spectrophotometer. UV-visible DRS electronic absorption spectrum was recorded using a Shimadzu-2600 spectrophotometer. TGA was carried out on an STA 409 PC Analyzer. PXRD plots were recorded on a Bruker D8-Advance diffractometer using graphite-

monochromated Cu $K\alpha_1$ (1.5406 Å) and $K\alpha_2$ (1.55439 Å) radiation.

4.2 Synthesis of **1**:

0.1037g (0.64 mmol) of 2, 2'-bipyridine was dissolved in 2 mL methanol followed by the addition of 50 mL water. To this solution, 15 mL glacial acetic acid was added and was stirred for 1 minute. To the stirred mixture, 1.4g (5.85 mmol) sodium molybdate was added and the resulting solution was kept for stirring. After 5 minutes, 0.5g (2.06 mmol) $\text{Cu}(\text{NO}_3)_2 \cdot 6\text{H}_2\text{O}$ was added followed by the addition of 1g (12.97 mmol) ammonium acetate. The resulting solution was then stirred for 1 hour at 70 °C. The reaction mixture was then filtered and the blue color filtrate was kept at room temperature to yield blue block crystals after four days. Yield: 0.8 g (20.3% based on Mo). FT-IR (cm^{-1}): 650, 700, 838, 895, 940, 1032, 1250, 1314, 1423, 1495, 1571, 2804, 3080, 3207, 3510. Elemental analysis (in %): Calculated: C: 15.29; H: 1.18; N: 2.97; Found: C: 14.89; H 1.2; N: 2.68.

4.3 Crystal Data Collection

X-ray reflections were collected on Bruker D8 QUEST, CCD diffractometer equipped with a graphite monochromator and Mo- $K\alpha$ fine-focus sealed tube ($\lambda = 0.71073$ Å), and the reduction was performed using APEX-II Software.³⁴ Intensities were corrected for absorption using SADABS, and the structure was solved and refined using SHELX97.³⁵ All non-hydrogen atoms were refined anisotropically. Hydrogen atoms on atoms were located from difference electron-density maps, and all C-H H atoms were fixed geometrically. Hydrogen-bond

geometries were determined in PLATON.³⁶ Crystal parameters are given in Table 1 and hydrogen bond distances are shown in Table S3 (SI). Selected bond lengths and bond angles of compound **1** are summarized in Table S2 (ESI). Crystallographic cif files (CCDC No. 1960325) are available at www.ccdc.cam.ac.uk/data or as part of the Supporting Information.

4.4 Electrochemical Studies

All electrochemical experiments were conducted using a Zahner Zammium electrochemical workstation operated by *Thales* software. Complete electrochemical experiments were accomplished using a three-electrode electrochemical cell with compound **1** modified glassy carbon as the working electrode, homemade Ag/AgCl (1 M) as the reference electrode and a Pt flag as the counter electrode in acidic pH in an aqueous medium. For the preparation of a **1**-modified electrode, 4 mg of **1** and 1 mg of acetylene carbon black were placed in a 1 mL of 3:2 mixture of ethanol/water and to it, was added 10 μL of 5 wt % Nafion (aqueous). The mixture was sonicated for 30 minutes to make it a homogeneous suspension. Then 5 μL of this mixture was coated on a 3-mm-diameter glassy carbon electrode (geometrical area = 0.0706 cm^2), resulting in 10 μg of the sample (compound **1**) in each coating on the glassy carbon electrode. The same amount on the electrode surface was maintained for all electrochemical experiments. The coating mixture on the electrode was dried under an IR lamp (temperature approx. 70 °C) prior to the experiment. All the experiments were conducted under ambient temperature. Electrode potentials were converted to the normal hydrogen

electrode (NHE) scale using the relationship $E(\text{NHE}) = E(\text{Ag}/\text{AgCl}) + 0.1263 \text{ V}$ as Ag/AgCl was used as the reference electrode. CV scans were initiated at the open-circuit potential and the anodic side was scanned first, followed by the cathodic side scan. Five cycles were taken consecutively for each set of CV measurements in the solution. Cyclic voltammograms were also recorded at various scan rates. For experiments in a non-aqueous medium, nitrogen gas was purged into the cell throughout the experiment.

Acknowledgments This work is supported by DST-SERB (project number: EMR/2017/002971) and the UGC-BSR project (project No. 19-232/2019(BSR)). We also acknowledge DST-FIST, UGC-SAP, and UPE-II for facilities. NTK thanks CSIR for fellowship. NTK thanks Ms. Chandani Singh and Mr. Subhabrata Mukhopadhyay for their help and valuable suggestions.

Keywords: Electrocatalytic H_2O_2 reduction, Electrocatalytic proton reduction, Electrocatalytic water oxidation, Polyoxometalates, Supramolecular interactions.

References

- (a) M. T. Pope, A. Muller, *Angew. Chem. Int. Ed.* 30 (1991) 34. (b) N. Mizuno, M. Misono, *Chem. Rev.* 98 (1998) 199. (c) U. Kortz, M. G. Savelieff, F. Y. A. Ghali, L. M. Khalil, S. A. Maalouf, D. I. Sinno, *Angew. Chem., Int. Ed.*, 41 (2002) 4070. (d) D. L. Long, E. Burkholder, L. Cronin, *Chem. Soc. Rev.*, 36, (2007) 105. (e) C. Y. Sun, S. X. Liu, D. D. Liang, K. Z. Shao, Y. H. Ren, Z. M. Su, *J. Am. Chem. Soc.* 131 (2009) 1883. (f) D. L. Long, R. Tsunashima, L. Cronin, *Angew. Chem., Int. Ed.*, 49 (2010) 1736.
- (a) C. Singh, S. Mukhopadhyay, S. K. Das, *Inorg. Chem.* 57 (2018) 6479. (b) X.-M. Li, Y.-G. Chen, T. Shi, *Solid State Sci.*, 52 (2016) 112. (c) M.-T. Li, J.-Q. Sha, X.-M. Zong, J.-W. Sun, P.-F. Yan, L. Li, X.-N. Yang, *Cryst. Growth Des.* 14 (2014) 2794. (d) C.-M. Liu, Y.-H. Huang, D.-Q. Zhang, F.-C. Jiang, D.-B. Zhu, *J. Coord. Chem.* 56 (2003) 953. (e) H. Wang, C. Cheng, Y. Tian, *Chin. J. Chem.* 27 (2009) 1099. (f) Y.-F. Li, D. G. Hubble, R. G. Miller, H.-Y. Zhao, W.-P. Pan, S. Parkin, B. Yan, *Polyhedron* 29 (2010) 3324. (g) Z. Yi, X. Zhang, X. Yu, L. Liu, X. Xu, X. Cui, J. Xu, *J. Coord. Chem.* 66 (2013) 1876.
- (a) Y. Xu, J.-Q. Xu, K.-L. Zhang, Y. Zhang, X. -Y. You, *Chem. Commun.* (2000) 153. (b) Y. Wang, B. Zou, L.-N. Xiao, N. Jin, Y. Peng, F.-Q. Wu, H. Ding, T.-G. Wang, Z.-M. Gao, D.-F. Zheng, X.-B. Cui, J.-Q. Xu, *J. Solid State Chem.* 184 (2011) 557. (c) J.-W. Cui, X.-B. Cui, H.-H. Yu, J.-Q. Xu, Z.-H. Yi, W.-J. Duan, *Inorg. Chim. Acta* 361 (2008) 2641. (d) R. N. Devi, E. Burkholder, J. Zubieta, *Inorg. Chim. Acta* 348 (2003) 150. (e) A. Dolbecq, E. Dumas, C. R. Mayer, P. Mialane, *Chem. Rev.* 110 (2010) 6009. (f) A. Kumar, A. K. Gupta, M. Devi, K. E. Gonsalves, C. P. Pradeep, *Inorg. Chem.* 56 (2017) 10325.

4. (a) V. McKee, M. Zvagulis, J. V. Dagdigian, M. G. Patch, C. A. Reed, *J. Am. Chem. Soc.*, 106 (1984) 4675. (b) T. N. Sorrell, M. L. Garrity, D. J. Ellis, *Inorg. Chim. Acta*, 166 (1989) 71. (c) R. N. Mukherjee, *Proc. Indian Natn. Sci. Acad.* 70 (2004) 329. (d) R. Novotna, Z. Travnicek, Herchel, *Bioinorg. Chem. Appl.* (2012) 704329.
5. M. Melink, M. Kabesova, M. Koman, L. Macaskova, J. Garaj, C. E. Holloway, A. Valent, *J. Coord. Chem.* 45 (1998) 147.
6. S. P. Perlepes, J. C. Huffman, G. Christou, *Polyhedron* 11 (1992) 1471.
7. S. Meenakumari, A. R. Chakravarty, *Polyhedron* 12 (1993) 347.
8. S. Reinoso, P. Vitoria, L. Lezama, A. Luque, J. M. Gutierrez-Zorilla, *Inorg. Chem.* 42 (2003) 3709.
9. S. Reinoso, P. Vitoria, J. M. Gutierrez-Zorilla, L. Lezama, L. S. Felices, J. I. Beitia, *Inorg. Chem.* 44 (2005) 9731.
10. S. Reinoso, P. Vitoria, L. S. Felices, L. Lezama, J. M. Gutierrez-Zorilla, *Chem. Eur. J.* 11 (2005) 1538.
11. S. Reinoso, P. Vitoria, L. S. Felices, L. Lezama, J. M. Gutierrez-Zorilla, *Inorg. Chem.* 45 (2006) 108.
12. S. Reinoso, P. Vitoria, J. M. Gutierrez-Zorilla, L. Lezama, J. M. Madariaga, L. S. Felices, A. Iturrospe, *Inorg. Chem.* 46 (2007) 4010.
13. H. Ma, L. Gong, F. Wang, X. Wang, *Struct. Chem.* 19 (2008) 435.
14. Q. X. Han, Y. M. Cheng, J. Li, J. P. Wang, *Russ. J. Coord. Chem.* 37 (2011) 547.
15. H. Pang, M. Yang, L. Kang, H. Ma, B. Liu, S. li, H. Liu, *J. Solid State Chem.* 198 (2013) 440.
16. S. Li, H. Ma, H. Pang, L. Zhang, Z. Zhang, *J. Mol. Struct.* 1063 (2014) 351.
17. J. Luo, P. Cheng, J. Zhao, L. Chen *Syn. React. Inorg. Metal-Org. Nano-metal Chem.* 45 (2015) 682-687.
18. Y. Hou, Y. Niu, C. Zhang, H. Pang, H. Ma, *J. Chem. Sci.* 129 (2017) 1639.
19. H. Miao, X. Xu, W. Ju, W. H. X. Wan, Y. Zhang, D. R. Zhu, Y. Xu, *Inorg. Chem.* 2014, 53, 2757-2759.
20. (a) A. Kudo, Y. Miseki, *Chem. Soc. Rev.* 38 (2009) 253. (b) M. D. Karkas, O. Verho, E. V. Johnston, B. Akermark, *Chem. Rev.* 114 (2014) 11863. (c) B. O'Regan, M. Gratzel, *Nature* 353 (1991) 737. (d) M. W. Kanan, D. G. Nocera, *Science*. 321 (2008) 1072. (e) R. D. L. Smith, M. S. Prevot, R. D. Fagan, Z. P. Zhang, P. A. Sedach, M. K. J. Siu, S. Trudel, C. P. Berlinguette, *Science* 340 (2013) 60. (f) S. Anantharaj, K. Karthick, S. Kundu, *Inorg. Chem.* 57 (2018) 3082.
21. C. Singh, S. Mukhopadhyay, S. K. Das, *Inorg. Chem.* 57 (2018) 6479.
22. (a) P. Cao, T. Fang, L. Z. Fu, L. L. Zhou, S. Z. Zhan, *Int. J. Hydrogen Energy* 39 (2014) 10980. (b) P. Zhang, M. Wang, Y. Yong, D. Zheng, K. Han, L. Sun, *Chem. Commun.* 50 (2014) 14153. (c) Y. Aimoto, K. Koshiba, K. Yamauchi, K. Sakai, *Chem. Commun.* 54 (2018) 12820. (d) K. Koshiba, K. Yamauchi, K. Sakai, *Dalton Trans.* 48 (2018) 635. (e) U. J. Kilgore, J. A. S. Roberts, D. H. Pool, A. M.

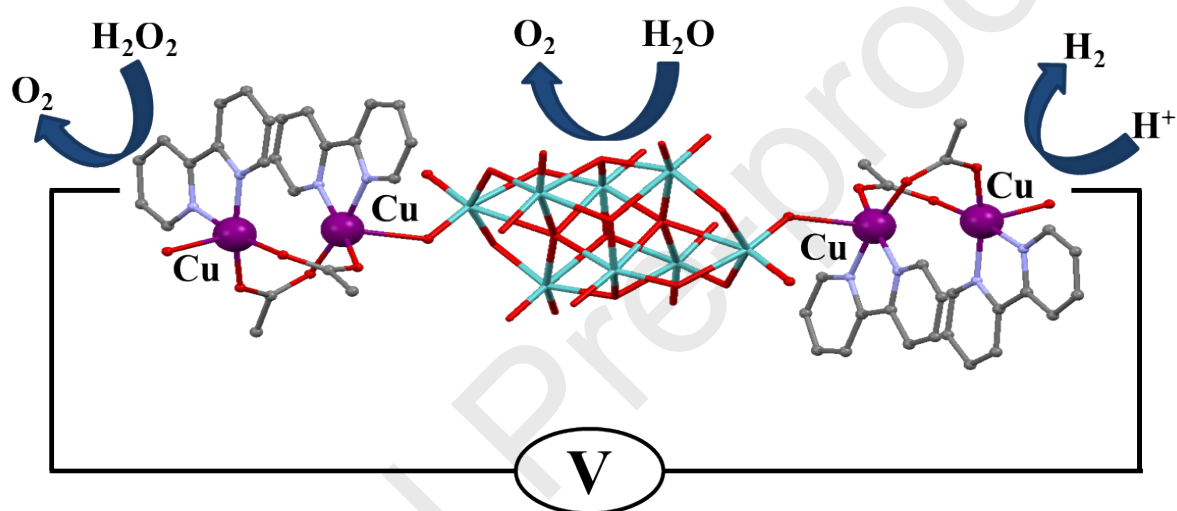
- Appel, M. P. Stewart, M. R. DuBois, W. G. Dougherty, W. S. Kassel, R. M. Bullock, D. L. DuBois, *J. Am. Chem. Soc.* 133 (2011) 5861. (f) S. Inoue, M. Mitsuhashi, T. Ono, Y.-N. Yan, Y. Kataoka, M. Handa, T. Kawamoto, *Inorg. Chem.* 56 (2017) 12129. (g) Y. Han, H. Fang, H. Jing, H. Sun, H. Lei, W. Lai, R. Cao, *Angew. Chem. Int. Ed.* 55 (2017) 5457.
23. (a) Y. Liu, L.-Z. Fu, L.-M. Yang, X.-P. Liu, S.-Z. Zhan, C.-L. Ni, *J. Mol. Catal. A: Chem* 417 (2016) 101. (b) H. Sun, Y. Han, H. Lei, M. Chen, R. Cao, *Chem. Commun.* 53 (2017) 6195. (c) J. Wang, C. Li, Q. Zhou, W. Wang, Y. Zhou, B. Zhang, X. Wang, *Catal. Sci. Technol.* 6 (2016) 8482. (d) X. Li, H. Lei, X. Guo, X. Zhao, S. Ding, X. Gao, W. Zhang, R. Cao, *ChemSusChem* 10 (2017) 4632. (e) H. Lei, A. Han, F. Li, M. Zhang, Y. Han, P. Du, W. Lai, R. Cao, *Phys. Chem. Chem. Phys.* 16 (2014) 1883. (f) X. Li, H. Lei, J. Liu, X. Zhao, S. Ding, Z. Zhang, X. Tao, W. Zhang, W. Wang, X. Zheng and R. Cao, *Angew. Chem. Int. Ed.* 57 (2018) 15070.
24. (a) B. Mondal and A. Dey, *Chem. Commun.* 53 (2017) 7707. (b) P. Du, R. Eisenberg, *Energy Environ. Sci.* 5 (2012) 6012. (c) A. Rana, B. Mondal, P. Sen, S. Dey, A. Dey, *Inorg. Chem.* 56 (2017) 1783.
25. (a) P. Zhang, M. Wang, Y. Yong, T. Yao, L. Sun, *Angew Chem Int. Ed.* 53 (2014) 13803. (b) T. Fang, L.-Z. Fu, L.-L. Zhou, S.-Z. Zhan, *Electrochimica Acta* 161 (2015) 388. (c) L.-L. Zhou, T. Fang, J.-P. Cao, Z.-H. Z., X.-T. Su, S.-Z. Zhan, *J. Power Sour.* 273 (2015) 298. (d) H. Lei, H. Fang, Y. Han, W. Lai, X. Fu, R. Cao, *ACS Catal.* 5 (2015) 5145.
26. C. Singh, S. K. Das, *Polyhedron* (2019) DOI: 10.1016/j.poly.2019.03.026.
27. A. J. Bridgeman, G. Cavigliasso, *Inorg. Chem.* 41 (2002) 3500.
28. (a) M. H. Rosnes, C. Yvon, D.-L. Long, L. Cronin, *Dalton Trans.* 41 (2012) 10071. (b) I. Zebiri, S. Boufas, S. Mosbah, L. Bencharif and M. Bencharif, *J. Chem. Sci.*, 127 (2015) 1769.
29. (a) N. E. Kuz'mina, K. K. Palkina, N. V. Polyakova, S. B. Strashnova, O. V. Koval'chukova, B. E. Zaitsev, A. N. Levov, *Russ. J. Coord. Chem.* 27 (2001) 711. (b) N. S. Bedowr, R. B. Yahya, N. Farhan, *J. Saudi Chem. Soc.* 22 (2018) 255.
30. (a) T. Yamase, *Chem. Rev.* 98 (1998) 307. (b) X. M. Zhang, B. Z. Shen, X. Z. You, H. K. Fun, *Polyhedron* 16 (1997) 95. (c) Y. Gong, C. Hu, h. Li, W. Tang, K. Huang, W. Hou *J. Mol. Struct.* 784 (2006) 228.
31. B. J. Coe, M. K. Peers, N. S. Scrutton, *Polyhedron* 96 (2015) 57.
32. (a) B. W. Koo *Bull. Korean Chem. Soc.* 22 (2001) 113. (b) A. B. P. Lever *Inorganic Electronic Spectroscopy*, 2nd Ed.; Elsevier, Amsterdam, (1984) 553-572, 636-638.
33. P. Wang, X. Wang and G. Zhu *Electrochim. Acta*, 46 (2000) 637.
34. Bruker SMART, Version 5.625, SHELXTL, Version 6.12; Bruker AXS Inc.: Madison, Wisconsin, USA, (2000).

35. G. M. Sheldrick, Program for Refinement of Crystal Structures; University of Göttingen, Germany, (1997).
36. (a) G. M. Sheldrick, Acta Crystallogr., Sect. A: Found. Crystallogr. 64 (2008) 112. (b) G. M. Sheldrick, Acta Crystallogr., Sect. C: Struct. Chem. 71 (2015) 3.

A Polyoxometalate Supported Copper Dimeric Complex: Synthesis, Structure and Electrocatalysis

N. Tanmaya Kumar, Umashish Bhoi and
Samar K. Das*

Art work for TOC



CRedit author statement

for the manuscript ICA_2019_1650

N. Tanmaya Kumar: Methodology, Visualization, Writing- Original draft preparation, Investigation. **Umashis Bhoi:** Investigation, Methodology. **Pragya Naulakha:** Software, Validation. **Samar K. Das:** Conceptualization, Visualization, Supervision, Reviewing and Editing.

Highlights.

- ▶ Polyoxometalate supported copper dimeric complexes. ▶ Crystal structure analysis. ▶ Spectral analysis. ▶ Electrocatalytic water oxidation and reduction. ▶ Electrocatalytic hydrogen peroxide reduction.